Influence of boundary reflection and refraction on diffusive photon transport

D. J. Durian
Department of Physics, University of California, Los Angeles, California 90024-1547
(Received 24 November 1993)

We report computer simulations which test the accuracy of the diffusion theories used in the analysis of multiple light scattering data. Explicitly including scattering anisotropy and boundary reflections, we find that the predicted probability for transmission through a slab is accurate to 1% if the slab thickness is greater than about 5 transport mean free paths. For strictly isotropic scattering and no boundary reflections, the exact diffusion theory prediction is accurate to this level for all thicknesses. In addition, we predict how the angular distribution of transmitted photons is affected by boundary reflectivity, both with and without refraction. Simulations show that, to a similar extent, corrections to diffusion theory from a more general transport theory are not needed here, either. Our results suggest an experimental means of measuring the so-called extrapolation length ratio which characterizes boundary effects, and thus have important implications for the analysis of static transmission and diffusing-wave spectroscopy data.

PACS number(s): 05.60.+w, 42.68.Ay, 07.60.Dq, 66.90.+r

I. INTRODUCTION

Dispersed forms of condensed matter such as colloids, foams, and emulsions all strongly scatter light so that even thin samples can appear white in the absence of absorption [1]. Many previously inaccessible aspects of their structure and dynamics are now being studied experimentally [2–9] with recent techniques, such as diffusing-wave spectroscopy [10,11] and interferometry [12], which exploit the diffusive nature of light propagation. Biological tissues also strongly scatter visible light, and efforts are underway to develop noninvasive medical probes [13,14] based on this feature. In addition, diffusive photon transport in general has been of interest for comparison with transport near the onset of localization [15]. In all cases, a crucial issue is the accuracy with which the propagation of multiply scattered light can be quantitatively described as a diffusion process. Here we address this issue in a simple yet experimentally important setting: the probability for an incident photon to be transmitted through an opaque, multiple scattering slab.

In all cases, a key quantity whose value must be known accurately is the transport mean free path l^*. This average distance required for complete randomization of the instantaneous propagation direction is related to the photon diffusion constant and propagation speed by $l^*=3D/c$; it can be thought of as the average step size in a random walk. For the ideal experimental case of a well-characterized suspension of colloidal spheres, the value of l^* may be computed from Mie scattering theory and the sphere number density. For other systems, where the scattering structure and form factors are not known *a priori*, the transport mean free path is commonly estimated from the probability that an incident photon will be transmitted through a sample of uniform thickness. To avoid the difficulties of absolute measurement, the usual procedure is to image a portion of the exiting light onto a detector for both the sample in question and also for a reference colloidal suspension. Since the transmission probability generally varies with sample thickness as $T \propto l^*/L$, the transport mean free path is estimated as $l^*=l_R^*(IL/I_RL_R)$, where I represents the detected intensity and the subscript R denotes the reference sample. This procedure can, however, be subject to unknown systematic errors from the exchange of samples and from unwarranted assumptions in the analysis. The latter include not only the accuracy of the diffusion approximation, but the sample independence of both the constant of proportionality between T and l^*/L, as well as the angular distribution of existing photons. To test the validity of these assumptions, we perform a series of random walk computer simulations which quantify the effects of finite slab thickness, anisotropic scattering, and the reflection and refraction of photons at the sample boundaries.

Our central result is that for slabs thick enough that essentially no ballistic photons are transmitted, the transmission probability for incident photons is described to the level of 1% by

$$T=\frac{1+z_e}{(L/l^*)+2z_e}\ , \tag{1.1}$$

where z_e, called the extrapolation length ratio, is a sample-dependent number of order unity which can be found for an unknown sample from analysis of the angular distribution of transmitted light. Our simulations also show that the extrapolation length ratio is more accurately predicted by conventional diffusion theory than by a modified version currently in wide use. These results are independent of anisotropy in the scattering form factor and have important implications for both the collection and analysis of multiple light scattering data.

In Sec. II we review the theoretical foundation for the functional form of Eq. (1.1) and the value of the extrapolation length ratio. In Sec. III we then systematically compare diffusion theory with computer simulation as a

function of system parameters. In Sec. IV we derive a simple prediction for the angular distribution of the exciting photons and confirm the accuracy of our result by computer simulation for the case of constant boundary reflectivity. When the Fresnel angle dependence of the boundary reflectivity is included, however, we find good agreement only for photons transmitted within about 45° of the surface normal. In the Appendixes we consider diffuse transmission in a continuum of arbitrary dimension and on various lattices.

II. DIFFUSION THEORY

The complete diffusion theory formalism within which the fraction T of normally incident photons transmitted through a slab of thickness L may be calculated is given by Ishimaru [1]. Ingredients include the diffusion equation, the source term, and the boundary conditions for the time-independent density $U(z)$ of photons at transverse distance z into the slab as measured from the incident edge. The flux of exiting photons is found by solving for $U(z)$ and evaluating its gradient at the boundaries. The source of diffusing photons is provided by photons scattered away from the incident beam and is assumed to decay as $\exp(-z/l_S)$, where l_S is the scattering mean free path of the medium. For the case of isotropic scattering, where the transport mean free path l^* equals the scattering mean free path l_S, the boundary conditions are

$$\left[U \mp h \frac{\partial U}{\partial z} \right]_{z=0,L} = 0 \ . \tag{2.1}$$

For the case of anisotropic scattering, where the transport mean free path is greater than the scattering mean free path according to an average of the angular deflection suffered in one scattering event, $l^* = l_S / \langle 1 - \cos\theta \rangle$, the boundary conditions are modified such that the right hand side of Eq. (2.1) is nonzero [1]. Note that the length h represents the distance outside the sample at which the density of isotropically scattering photons vanishes; it is therefore called the extrapolation length. The dimensionless extrapolation length ratio, as appears in Eq. (1.1), is $z_e \equiv h/l^*$; its value is $\frac{2}{3}$ in Ishimaru's diffusion theory, but is affected by the reflectivity of the boundary walls. By setting the fictional flux of diffuse photons entering the sample to an average boundary reflectivity R times the diffuse flux of photons leaving the sample, Zhu, Pine, and Weitz [16] predict that the extrapolation length ratio is more generally given by

$$z_e = \frac{2}{3} \frac{1+R}{1-R} \ . \tag{2.2}$$

This reduces to Ishimaru's result when there are no boundary reflections; for realistic values of R, however, the extrapolation length can be two or three times larger. In Appendix A we generalize for a d-dimensional continuum and find that only the numerical prefactor in Eq. (2.2) changes.

Ishimaru's diffusion theory can be exactly solved for a slab of arbitrary thickness and scattering anisotropy. We find that the density of diffusing photons normalized by the value at the incident wall is

$$\frac{U(z)}{U(0)} = 1 + \frac{1 - \exp(-z/l_S) - zT/l^*}{z_e(1-T)} \ , \tag{2.3}$$

where T is the total transmission, or fraction of incident photons which are transmitted through the sample. For the case $l^* = l_S = L/10$ the photon density is plotted in Fig. 1; tangent lines at $z=0$ and L are included to demonstrate the extrapolation length boundary conditions of Eq. (2.1). The total transmission T is the sum of a "ballistic" contribution $T_B = \exp(-L/l_S)$ from photons which remain unscattered from the incident beam and a "diffuse" contribution given by

$$T_D = \frac{[1+z_e] - [1+z_e+L/l^*]\exp(-L/l_S)}{(L/l^*)+2z_e} \ . \tag{2.4}$$

For isotropic scattering, expansion of Eq. (2.4) gives the correct result in the limit of thin slabs, $L \ll l^*$, in which incident photons scatter at most once: In this single scattering regime the diffuse transmission varies with thickness as $T_D \approx L/2l^*$, since the fraction of incident photons which scatter is $1 - T_B \approx L/l^*$ and the fraction of those which scatter into the forward direction is $\frac{1}{2}$. For anisotropic scattering and very thin slabs, however, the diffusion theory prediction of Eq. (2.4) cannot in principle be correct since the fraction scattered forward is greater than the fraction scattered backward according to details of the scattering form factor which cannot be included in a diffusion theory. Indeed, for sufficiently anisotropic scattering and small thicknesses, the sum of ballistic and diffuse transmission probabilities given above by diffusion theory can be greater than one, which is blatantly and dramatically incorrect.

In this paper, we are more concerned with transmission through opaque slabs which are sufficiently thick

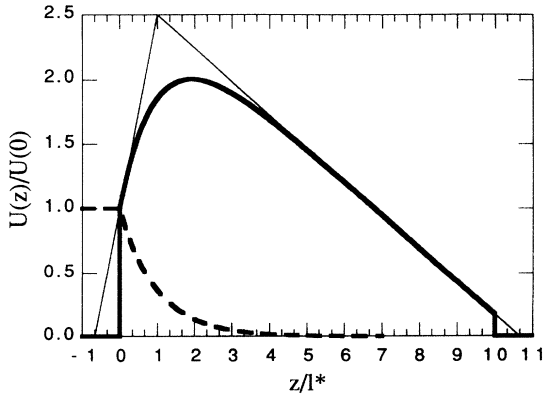

FIG. 1. Diffuse [Eq. (2.3), bold curve] and ballistic (dashed curve) photon density vs transverse distance across a slab which is ten transport mean free paths thick, $L/l^* = 10$, for the case of isotropic scattering and zero boundary reflectivity. The thin lines tangent to the diffuse photon density at $z=0$ and L, respectively, intersect at $z = l^*$ and go to zero at $h = z_e l^*$ outside the sample, where $z_e = \frac{2}{3}$ is called the extrapolation length ratio.

that essentially no ballistic photons are transmitted. In this limit $T_B \ll T_D$, the exponential term in Eq. (2.4) is negligible and the simple algebraic form of Eq. (1.1) is recovered. For such opaque slabs, the predicted transmission has no direct dependence on scattering anisotropy; the only two relevant lengths are the cell thickness and the transport mean free path. For extremely thick slabs, the transmission follows an Ohm-like law L^{-1} with a constant of proportionality which depends on the extrapolation length ratio and hence on the boundary reflections. For thinner opaque slabs, Eq. (1.1) provides corrections to strict Ohm-like behavior.

Though Eq. (1.1) was derived above from the full diffusion theory formalism of Ishimaru and can also be derived using Green's function techniques assuming a point source of isotropically scattering photons located at exactly $z=l^*$ [17], the functional form has a simple physical interpretation. Away from source terms, the steady state diffuse photon density must vary linearly with transverse position since $\partial^2 U/\partial z^2=0$. The density would therefore decrease linearly in both transverse directions away from a source at $z=l^*$ in such a way as to reach zero at $z_e l^*$ outside the sample; in other words, it would behave like the tangent lines in Fig. 1. The diffusely transmitted and backscattered fluxes must then be $J_T \propto (L+z_e l^*-l^*)^{-1}$ and $J_B \propto (z_e l^*+l^*)^{-1}$, respectively, since the flux is proportional to the density gradient. This gives the diffuse transmission probability as $T_D=J_T/(J_T+J_B)$, which reproduces Eq. (1.1) exactly.

The functional form of Eq. (1.1) is even more robust than diffusion theory, as we further demonstrate with a third derivation assuming *only* that photons execute a random walk which starts at $z=l^*$ and stops at either $z_B=-z_e l^*$ or $z_T=L+z_e l^*$ for backscattering and transmission, respectively. Since a photon that reaches the center of the sample will have equal probability of being backscattered or transmitted, we must have $T_D(L)=T_D(L')/2$, where L' is given by $L'+2z_e l^* = (L+2z_e l^*)/2$. Repeating n times gives $T_D(L) = T_D[(L+2z_e l^*)/2^n - 2z_e l^*]/2^n$ and stopping the recursion with $T_D(2l^*)=\frac{1}{2}$ yields Eq. (1.1) exactly.

While the functional form of Eq. (1.1) for transmission is thus on very firm theoretical ground, the concept of an extrapolation length for the average photon density, let along the value predicted by Eq. (2.2), is not. An unwarranted assumption implicit in diffusion theory is that diffusing photons can be described merely by their local concentration, as though their velocity distribution were isotropic everywhere in the sample. A more general transport theory that relaxes this assumption is the theory of radiative transfer, which provides an analytical formalism for calculation of the density $U(z,\mu)$ of photons at z traveling at an angle $\cos^{-1}(\mu)$ from the $+z$ direction [18]. For example, note that diffusion theory cannot describe the introduction of photons anisotropically scattered from an incident beam, nor can it account for photon transport within roughly one transport mean free path of the sample boundary; the more general radiative transfer theory is needed for analytical description of such phenomena. Radiative transfer theory can, in addition, be applied to a wide variety of transport phenomena where boundary reflections play a role, such as for phonons in a crystal [19,20], molecules in a rarefied gas [21,22], and of course photons in a highly scattering medium [23]. The so-called Milne problem of astrophysics is to calculate $U(z,\mu)$ for the case of steady flux emerging from a semi-infinite medium. This is intended to mimic photons emerging from the sun, as well as neutrons emerging from a reactor. The result is that the following second moment of U possesses an extrapolation length [24]:

$$\int_{-1}^{1} U(z,\mu)\mu^2 d\mu \propto (z/l^*)+z_0 \ . \tag{2.5}$$

The value of the Milne extrapolation length ratio is $z_0 \cong 0.7104$, which is, of course, on the order of unity and happens to be numerically close to the diffusion theory extrapolation length ratio of $\frac{2}{3}$ even though the two have different physical meanings.

Recently, a modified diffusion theory has been proposed in which the Milne extrapolation length ratio is used instead of $\frac{2}{3}$ in the otherwise standard diffusion theory formalism [25]; the intention is to increase the accuracy of diffusion theory without sacrificing its analytical simplicity. This minor change would be more appealing conceptually if radiative transfer theory had predicted that the average photon density, rather than the second moment in Eq. (2.5), extrapolates to zero outside the sample. Reference [25] includes a computer simulation purported to justify the modification of diffusion theory; the transmission probability for four different slab thicknesses $L/l^* \cong 3$, 5, 11, and 32 is found to be described by

$$T=\frac{0.8126}{0.7034(L/l^*)+1}=\frac{1+0.1552}{(L/l^*)+2\times 0.7108} \ . \tag{2.6}$$

We have rewritten the result for direct comparison with Eq. (1.1). Note that only the term responsible for small-thickness corrections gives an effective extrapolation length ratio close to the Milne value; the leading behavior gives an entirely different number. Nevertheless, the modified diffusion theory is widely used in analyzing experimental data [17,26] and proponents argue that 0.7104 should be the numerical prefactor used in Eq. (2.2).

III. TRANSMISSION SIMULATION

In order to definitively settle the issue of the numerical prefactor in Eq. (2.2) and to generally examine the accuracy of the diffusion theory prediction Eq. (1.1) for the transmission through an opaque multiple scattering slab, we perform a series of random walk computer simulations. While in principle it may be possible to use radiative transfer theory to analytically account for deviations of diffusion theory from simulation results, our interest is rather to directly assess the applicability and accuracy of diffusion theory as it is currently widely used in analysis of experimental data. Also, since localization and other interference phenomena are not included, our results could help to distinguish wave effects from transport effects in experimental situations.

A. Isotropic scattering, no boundary reflectivity

The simplest random walk model of transport through a slab is one where the propagation direction of an individual photon is completely randomized at each scattering event and where boundary reflections are not allowed. In our first simulation, then, successive photons are launched in the $+z$ direction starting from $z=0$ and are allowed to wander by a series of scattering events, or steps, until exiting at either $z=0$ or L. To generate such walks one step at a time, we keep track of the current position and take a new step whose size and direction, respectively, are

$$\Delta s = -l^* \ln \mathcal{N}_{\text{rand}}, \quad \mu = 2\mathcal{N}_{\text{rand}} - 1 , \tag{3.1}$$

where $\mathcal{N}_{\text{rand}}$ is a random number between zero and one and $\theta = \cos^{-1}(\mu)$ is the angle between the propagation and $+z$ directions. The corresponding change in transverse coordinate of the photon's position is $\Delta z = \mu \Delta s$. Note that the step length is variable and that the stepping rule in Eq. (3.1) ensures that the unscattered intensity falls off exponentially with distance in comparison with the transport mean free path. The direction rule ensures that the scattering is isotropic, since in three dimensions the infinitesimal solid angle element is $d\Omega = \sin\theta\, d\theta\, d\varphi = -d\mu\, d\varphi$ and the azimuthal angle φ has no influence on transverse position.

We compute the ballistic and diffuse transmission probabilities from the fraction of random walks transmitted through a slab with and without scattering. The statistical uncertainty improves with the total number of transmitted and backscattered walks according to

$$\Delta T = T(1-T)[N_T^{-1/2} + N_B^{-1/2}] . \tag{3.2}$$

For thin slabs in which there is only very rarely more than one scattering event, the run time required for a given number of diffuse transmission events, and hence a given level of uncertainty in the diffuse transmission, scales with slab thickness as L^{-1} since the diffuse transmission is proportional to L. For thick slabs in the multiple scattering regime, by contrast, the required time scales as L^2 since the average number of steps per transmission scales as $(L/l^*)^2$. Accordingly, good statistics are acquired most quickly for slab thicknesses on the order of one transport mean free path, and it is far more time consuming to simulate the multiple scattering regime. Note that to improve ΔT by a factor of 10, for example, requires an increase in runtime of 100.

Simulation results for the diffuse transmission probability in the case of isotropic scattering and no boundary reflections are plotted in Fig. 2 for slab thicknesses varying over six orders of magnitude, from the single scattering regime to deep into the multiple scattering regime. For thicknesses in the range $0.001 \le L/l^* \le 100$, each data point is based on either 10^6 or 2×10^6 diffuse transmission events and the statistical uncertainty is approximately 0.1%. For thicker slabs, the number of diffuse transmission events decreases roughly as a factor of 3 for every factor of 2 increase in L/l^* and the uncertainty blooms to 1% at $L/l^* = 1000$; better statistics were impractical to achieve. Over the entire range of

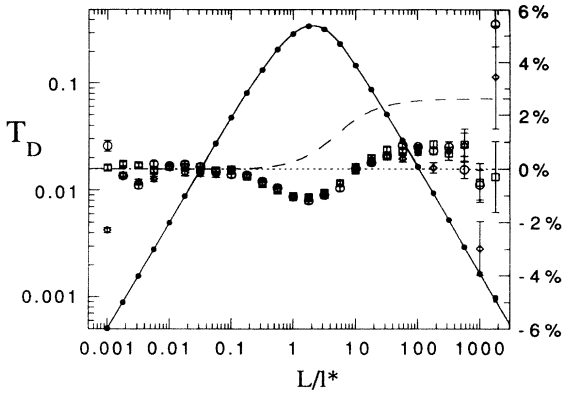

FIG. 2. Diffuse transmission (left) vs slab thickness for isotropic scattering and zero boundary reflectivity. The diffusion theory prediction [Eq. (2.4), solid curve] is indistinguishable from simulation results on this scale. The percent deviation of simulation data (open symbols) and modified diffusion theory (dashed) from Eq. (2.4) is shown on the right; error bars indicate counting uncertainty. The different symbols distinguish runs designed to test for the presence of systematic errors.

L/l^* examined, we find good, but not perfect, agreement with the diffusion theory prediction of Eq. (2.4) where the extrapolation length ratio is $z_e = \frac{2}{3}$. In particular, the deviation plotted on the right axis becomes systematic outside the single scattering regime, but is never more than about 1%. Note that the small statistical uncertainty in our data is crucial for the observation of this deviation. It is perhaps surprising that diffusion theory works well even for slabs on the order of one transport mean free path in thickness, where an anisotropic velocity distribution would be expected throughout the entire sample.

We stress that the comparison in Fig. 2 is made using $\frac{2}{3}$ as the extrapolation length ratio; had 0.7104 been used, the dashed curve on the right axis in Fig. 2 demonstrates that the deviation would be greater. Straight diffusion theory therefore more accurately describes photon transport than the modified diffusion theory discussed earlier. If one wishes to modify diffusion theory by altering the extrapolation length ratio, the value most consistent with our simulation is found by inverting the transmission data using Eq. (2.4) and computing a weighted average and statistical uncertainty. This gives $z_e = 0.673 \pm 0.002$ with normalized average square deviation $\chi^2 = 20$; evidently, Eq. (2.4) cannot truly describe our data to better than about 1%. Nevertheless, the value we find for z_e is significantly closer to $\frac{2}{3}$ than 0.7104, which again shows that straight diffusion theory is superior to the modified diffusion theory of Ref. [25]. If the 1% accuracy level of diffusion theory is not as great as desired in an analytical theory, then recourse to radiative transfer theory is recommended.

As a technical note, we discuss possible systematic errors in the simulation data of Fig. 2. More perhaps as a check on our computer code, we first confirm that the ballistic transmission results vary as $T_B = \exp(-L/l^*)$ to within statistical uncertainty for $0.001 \le L/l^* \le 10$; for thicker slabs no ballistic transmission events are ob-

served. This check is reflected less stringently in the diffuse transmission in the single scattering regime shown in Fig. 2, where $T_D=(1-T_B)/2\approx L/2l^*$ is observed as expected [see the discussion immediately following Eq. (2.4)]. To test for the effect of sequential correlations or other nonrandom behavior in our code, we employ two qualitatively different random number generators: a system-supplied ANSI-C conformant linear congruential generator, plotted as circles in Fig. 2, and the RAN3 subtractive generator published in [27], plotted as squares; the results are indistinguishable. This further eliminates the finite number of possibilities for $\mathcal{N}_{\text{rand}}$ in Eq. (3.1) as a source of systematic error, because the system-supplied routine and RAN3 respectively produce 32 767 and 10^9 different numbers. Next, the simulation results plotted as squares in Fig. 2 represent a run using the system-supplied generator, but where all lengths are scaled by l^* rather than by L as in the other two cases. This third run involves one less multiplication per random step and so should accumulate less roundoff error in the walker's instantaneous position; since all runs show identical behavior, such roundoff cannot be important. Finally we note that roundoff error in the transmission computation is easily made insignificant by use of long integers and double precision floating point numbers. Based on these tests, we conclude that counting uncertainty is the most significant error in our simulation data.

B. Angle-independent boundary reflectivity

Next, we incorporate into our code the possibility for photons to occasionally reflect from the sample boundaries in order to test the accuracy of the Zhu-Pine-Weitz diffusion theory boundary condition Eq. (2.2). In general, external boundary reflections can be expected to occur in experimental systems [11,28,29], and Eq. (2.2) suggests that even modest average diffuse reflectivities can substantially increase the value of the extrapolation length and hence affect analysis of transmission data in terms of the transport mean free path. The simplest simulation that includes this effect is to take the diffuse boundary reflectivity R as constant, independent of the angle with which the photon strikes the surface. In our simulation we thus compare a random number generated between zero and one with R whenever a boundary is encountered; if it is less than R the photon exits, otherwise, it reflects specularly and its new transverse position is taken inside the sample so that the step length is unaltered. Simulation results for the diffuse transmission are shown in Fig. 3 for 20 values of R ranging between 0 and 0.95 and a variety of slab thicknesses. Note that the transmission increases with increasing boundary reflectivity; to neglect boundary reflections in the analysis of actual experimental data would cause the transport mean free path to be systematically overestimated. For comparison with diffusion theory, the predictions of Eqs. (1.1) and (2.2) are included in Fig. 3 as solid curves. The agreement is evidently very good over the entire range of R and for sample sufficiently thick that essentially no ballistic photons are transmitted. For thinner samples, the deviation actually decreases as R increases, but cannot be seen in the plot. To quantify the comparison, we use Eq. (1.1) to invert transmission data with $L \geq 10l^*$ for the numerical prefactor in Eq. (2.2). The weighted average of this bare extrapolation length ratio is found to be 0.665 ± 0.005 with $\chi^2=0.55$; with $\chi^2=0.55$; therefore our simulation results are consistent with diffusion theory and the full boundary condition of Zhu, Pine, and Weitz at the level of 1%.

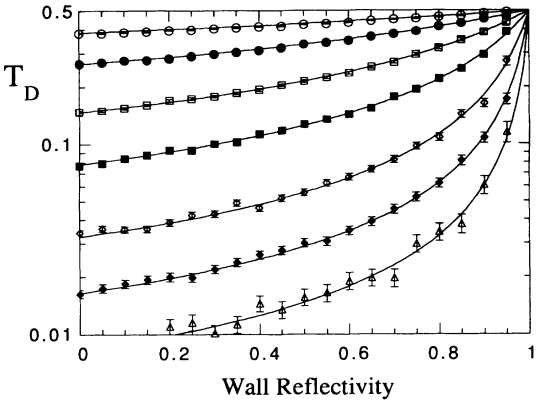

FIG. 3. Diffuse transmission vs wall reflectivity; comparison of Eqs. (1.1) and (2.2) with random walk simulations results for the case of isotropic scattering. From top to bottom, the slab thicknesses are $L/l^*=3$, 5, 10, 20, 50, 100, and 200.

C. Anisotropic scattering

In order to further test the general validity of Eqs. (1.1) and (2.2), we conduct a set of transmission simulations which relax the assumption of isotropic scattering. This is an important issue not only because scattering is preferentially in the forward direction for most scattering materials, but because the derivation of the diffusive boundary condition Eq. (2.2) explicitly assumes that the scattering is isotropic. For anisotropic scattering, the right hand side of Eq. (2.1) is nonzero and the concept of an extrapolation length seems to be ill defined. To simulate the effects of scattering anisotropy, we choose the simplest possible scattering form factor, namely a fixed angular deviation θ_F from the direction of the previous step. The size of a new step and the azimuthal angle about the previous step direction are respectively taken to be

$$\Delta s=-l_S \ln\mathcal{N}_{\text{rand}}, \quad \varphi=2\pi\mathcal{N}_{\text{rand}} . \tag{3.3}$$

This ensures that the unscattered intensity falls off exponentially in comparison with the scattering length l_S and that the transport mean free path is given by $l^*=l_S/(1-\cos\theta_F)$. By straightforward geometry, the change in coordinates of the photon position is

$$\Delta x=\frac{\Delta s}{\Delta s_0}\left[\cos\theta_F\Delta x_0-\sin\theta_F\cos\varphi\frac{\Delta x_0\Delta z_0}{\sqrt{\Delta x_0^2+\Delta y_0^2}}+\sin\theta_F\sin\varphi\frac{\Delta s_0\Delta y_0}{\sqrt{\Delta x_0^2+\Delta y_0^2}}\right],$$

$$\Delta y=\frac{\Delta s}{\Delta s_0}\left[\cos\theta_F\Delta y_0-\sin\theta_F\cos\varphi\frac{\Delta x_0\Delta z_0}{\sqrt{\Delta x_0^2+\Delta y_0^2}}-\sin\theta_F\sin\varphi\frac{\Delta s_0\Delta x_0}{\sqrt{\Delta x_0^2+\Delta y_0^2}}\right], \tag{3.4}$$

$$\Delta z=\frac{\Delta s}{\Delta s_0}[\cos\theta_F\Delta z_0+\sin\theta_F\cos\varphi\sqrt{\Delta x_0^2+\Delta y_0^2}\,],$$

where the subscript 0 denotes the previous step specifications. With these rules, simulation results for the transmission as a function of R are presented in Fig. 4 for nine distinct sets of slab thickness and scattering anisotropy: $L/l^*=5$, 10, and 20 combined with $l^*/l_S=2$, 5, and 10. The diffusion theory predictions are included as solid curves. Not only are the simulation results at a given L/l^* independent of scattering anisotropy to within statistical uncertainty, but they agree very well with the predictions shown. Analyzing transmission data in terms of the numerical prefactor in Eq. (2.2) gives a bare extrapolation length ratio marginally consistent with diffusion theory: 0.676 ± 0.008 with $\chi^2=0.64$. Anisotropy therefore has no effect on diffuse transmission for opaque slabs, even in the presence of boundary reflections, at the 1% level.

D. Angle-dependent boundary reflectivity

For the remainder of Sec. III, we address our previous simplification that the boundary reflectivity is independent of angle; this is done for a few special cases relevant for multiple light scattering experiments on samples contained in glass cells where photons may reflect or refract at either the sample-glass or glass-exterior interfaces according to the Fresnel laws [30]. Since actual cell walls are always much thicker than the wavelength of visible light, we assume that multiply reflected rays add incoherently, in the spirit of radiative transfer. Summing the intensities gives the angular dependent reflectivity of the entire boundary as

$$R(\mu)=\frac{R_{12}+R_{23}-2R_{12}R_{23}}{1-R_{12}R_{23}}, \tag{3.5}$$

where R_{ij} is the polarization-averaged Fresnel reflectivity of the ij interface when a photon strikes the boundary at an angle $\cos^{-1}(\mu)$ from the normal. The average diffuse reflectivity R, which determines the extrapolation length ratio in Eq. (2.2), is given by Zhu, Pine, and Weitz as

$$R=\frac{3C_2+2C_1}{3C_2-2C_1+2},\quad C_n=\int_0^1 R(\mu)\mu^n d\mu\,. \tag{3.6}$$

Numerical results for R, and the corresponding prediction for the extrapolation length ratio, are shown in Table I for six cases of experimental interest: where the sample has refractive index $n_1=1.33$ or 1, for aqueous suspensions and foams, respectively; where the cell walls have refractive index $n_2=1.52$ or 1.46, for Pyrex and quartz, respectively; and where the exterior of the cell has refractive index $n_3=1$, or 1.33, with the latter being for immersion in a water bath. Reflections from a second interface have not been considered previously [16,23]; however, the predictions in Table I would be substantially different had we also assumed $R_{23}=0$. Note that changing the cell wall material from Pyrex to quartz affects the extrapolation length ratio by roughly 3%.

The predictions in Table I can be tested by comparison with random walk simulations in which the probability for reflection at the boundary is now taken from Eq. (3.5); we consider only the case of Pyrex cell walls and isotropic scattering. Analyzing transmission results for cells of thickness $L/l^*=5$, 10, 20, 40, and 160 in terms of Eqs. (1.1) and (2.2) gives the bare extrapolation length ratios shown in Table I. For all three refractive index profiles, agreement with the diffusion theory prediction is perfect to almost three significant figures. Once again we find that straight diffusion theory is not in need of corrections from the full theory or radiative transfer; furthermore, we recommend the extrapolation length ratios in Table I as the most accurate available for analysis of experimental data on the specified systems.

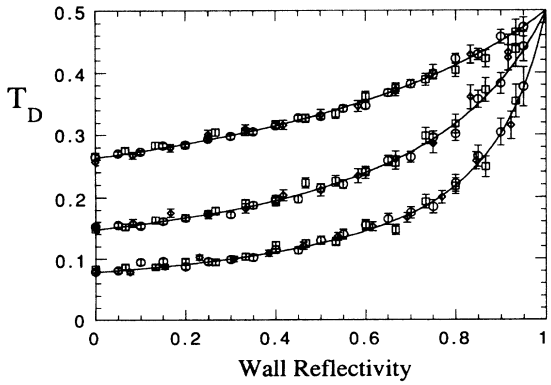

FIG. 4. Diffuse transmission vs wall reflectivity; comparison of Eqs. (1.1) and (2.2) with random walk simulation results for three different scattering anisotropies $l^*/l_S=2$, 5, and 10 (circles, squares, and diamonds, respectively). From top to bottom, the slab thicknesses are $L/l^*=5$, 10, and 20.

TABLE I. Diffusion theory predictions and simulation results for the extrapolation length ratio in several cases of experimental interest. Boundary reflections are due to refractive index mismatch between the interior (n_1), cell wall (n_2), and exterior (n_3) of the sample.

n_1	n_2	n_3	R	z_e prediction	z_e simulation
1.33	1.52	1	0.452 2	1.768	1.779±0.013
1.33	1.46	1	0.445 3	1.737	
1.33	1.52	1.33	0.042 44	0.7258	0.7284±0.0059
1.33	1.46	1.33	0.029 77	0.7076	
1	1.52	1	0.131 7	0.8785	0.8771±0.0040
1	1.46	1	0.123 0	0.8536	

IV. ANGULAR DISTRIBUTION

A. Theory

Now that the accuracy of the diffusion theory prediction Eqs. (1.1) and (2.2) for the transmission through an opaque multiple scattering slab of arbitrary boundary reflectivity and scattering anisotropy is known to be about 1%, the issue that remains is how to determine the extrapolation length ratio for an experimental sample. In this section, we show how to extract such information from the functional form of the angular distribution of transmitted photons. Consider the diffusive flux exiting through an area element dA and within a solid angle $d\Omega$ centered at angle θ from the normal. Assuming isotropic scattering and that the photon density has an extrapolation length h, we estimate the probability that an exiting photon lies within this solid angle by integrating over the corresponding space inside the sample:

$$J \propto \int_0^\infty [(h+r\cos\theta)r^2 dr\, d\Omega]\frac{dA\cos\theta}{r^2}\exp(-r/l^*) . \tag{4.1}$$

The term in square brackets is proportional to the number of photons in a volume element at a distance r away from dA and $r\cos\theta$ from the surface; the next term is proportional to the fraction of those photons headed toward dA; and the exponential term is the fraction of those which reach dA without scattering and therefore exit. The integral over r, which is easily performed, gives the total diffusive flux into $d\Omega$. Since there is azimuthal symmetry, we normalize our result in terms of the probability $P(\mu)d\mu$ that an exiting photon strikes the interior surface at an angle between $\cos^{-1}(\mu)$ and $\cos^{-1}(\mu+d\mu)$ from the normal:

$$P(\mu)=\frac{z_e\mu+\mu^2}{z_e/2+1/3} . \tag{4.2}$$

In contrast with Lambert's cosine law [30], we predict the angular distribution of diffusely transmitted light to be a mixture of cosine and cosine-squared terms which depends on the value of the extrapolation length ratio. Physically, the origin of the cosine term is that a given photon must travel further through the scattering medium in order to exit at a larger angle from the normal and hence is more likely to scatter before reaching the surface. The origin of the cosine-squared term is this first effect convoluted with the linear increase in photon density with depth as controlled by the extrapolation length ratio.

Note also that Eq. (4.2) is the proper form with which to compare experimental data taken by moving a detector of area D^2 in a circle of radius R_D about the sample: The detected intensity is

$$I=I_T\left[P(\mu)\sin\theta\frac{D}{R_D}\right]\left[\frac{D}{2\pi R_D\sin\theta}\right]=\left[\frac{I_T D^2}{2\pi R_D^2}\right]P(\mu) , \tag{4.3}$$

where I_T is the total transmitted intensity, the next term is $P(\mu)d\mu$, and the last term is the azimuthal fraction of photons transmitted between $\cos^{-1}(\mu)$ and $\cos^{-1}(\mu+d\mu)$ which fall on the detector. The detected intensity thus equals a constant times $P(\mu)$. A critical way to judge the functional form of the angular distribution is by inspecting the linearity $P(\mu)/\mu$ vs μ; this also provides a simple means of estimating z_e from the best fit to a line [31].

B. Simulation

Since the angular distribution in Eq. (4.2) was derived within diffusion theory assuming both isotropic scattering and the existence of an extrapolation length for the average diffuse photon density, we perform a series of simulations to test its accuracy. Our previous routines are simply modified to first bin up exiting photons according to the cosine of their exit angle and then to normalize by the total number transmitted. In Fig. 5 we compare the prediction of Eq. (4.2) with simulation results for fixed cell thickness $L=15l^*$, two wall-reflectivities $R=0$ and $\frac{1}{2}$, and five different scattering form factors: isotropic and fixed angle such that $l^*/l_S=3$, 10, 30, and 90. In all cases, $P(\mu)/\mu$ is found to be nearly linear in μ, especially near the normal direction $\mu=1$ where the agreement with Eq. (4.2) is excellent. For exiting angles further from the normal than about $\cos^{-1}(0.5)=60°$, the deviation of the simulation data from prediction, though noticeable, becomes striking only for highly anisotropic scattering. Additional simulation runs for different thicknesses $L/l^*=10$ and 20 and diffuse reflectivities $R=0.25$ and 0.75 are found to agree similarly well with our prediction Eq. (4.2). Therefore, the arguments leading to Eq. (4.2) quantitatively capture the essential physics for the angular distribution of photons transmitted through an opaque multiple scattering medium.

Another effect that influences the angular distribution is refraction. The exit angle θ_e for photons striking the

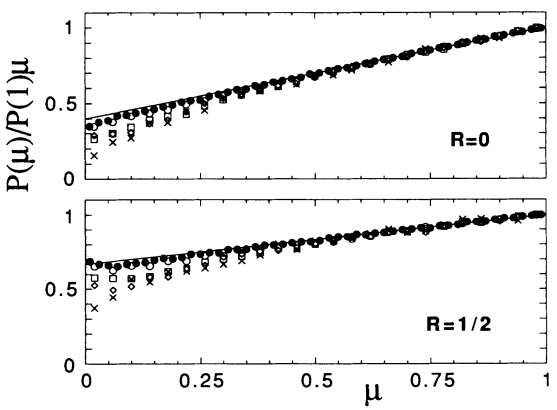

FIG. 5. Angular distribution of photons transmitted through slabs of thickness $L/l^*=15$ and different boundary reflectivities as labeled. Solid circles are for isotropic scattering; open circles, squares, diamonds, and crosses are, respectively, for fixed-angle anisotropic scattering with $l^*/l_S=3$, 10, 30, and 90. The solid lines represent the diffusion theory prediction, Eq. (4.2) with extrapolation length ratios given by Eq. (2.2).

interior boundary at angle θ is given by Snell's law $n_1 \sin\theta = n_3 \sin\theta_e$, where n_1 and n_3 are the interior and exterior refractive indices, respectively, as introduced in Sec. III D. Considering the change in solid angle upon refraction and assuming that Eq. (4.2) describes the distribution with which photons strike the interior surface, we find that the normalized probability density for the cosine of the angle with which they emerge is

$$\frac{P(\mu_e)}{\mu_e} = \frac{z_e + \left[1 - \frac{n_3^2}{n_1^2}(1-\mu_e^2)\right]^{1/2}}{\frac{1}{2}z_e + \frac{1}{3}\frac{n_1^2}{n_3^2}\left[1 - \left[1 - \frac{n_3^2}{n_1^2}\right]^{3/2}\right]} . \quad (4.4)$$

When there is refraction at the cell walls, therefore, we expect $P(\mu_e)/\mu_e$ to be strictly linear in μ_e only if the sample interior and exterior have the same refractive indices, in which case Eq. (4.2) is recovered. Expansion of Eq. (4.4) for photons exiting close to the surface normal helps reveal the influence of refraction:

$$\frac{P(\mu_e)}{P(1)\mu_e} = 1 - \frac{n_3^2}{n_1^2}\frac{(1-\mu_e)}{(1+z_e)} + \frac{n_3^2}{n_1^2}\left[1 - \frac{n_3^2}{n_1^2}\right]\frac{(1-\mu_e)^2}{2(1+z_e)} + O((1-\mu_e)^3) . \quad (4.5)$$

The second order term is small unless there is a substantial index mismatch, so nearly linear behavior may ordinarily be expected.

The prediction of Eq. (4.4) can be tested by comparison with random walk simulation of the angular distribution of exiting photons for the experimentally relevant refractive index profiles considered in Sec. III D. In Fig. 6 we show three such comparisons for the case of $L/l^* = 15$ and isotropic scattering. We find that $P(\mu_e)/\mu_e$ is linear in the vicinity of $\mu_e = 1$, as expected, and that this leading behavior is well described by Eq. (4.4). Further away from the normal direction than about $\cos^{-1}(0.7) \approx 45°$, however, we find that $P(\mu_e)/\mu_e$ decreases significantly faster than linearly in μ_e, in clear disagreement with our diffusion theory prediction. Indeed, for two of the cases shown the interior and exterior indices are the same and exactly linear behavior was expected; for the other case, the observed deviation from linearity is in the opposite direction from Eq. (4.4). While an analytical explanation of these results may perhaps be found using radiative transfer theory, the leading behavior can nevertheless be well understood by straight diffusion theory.

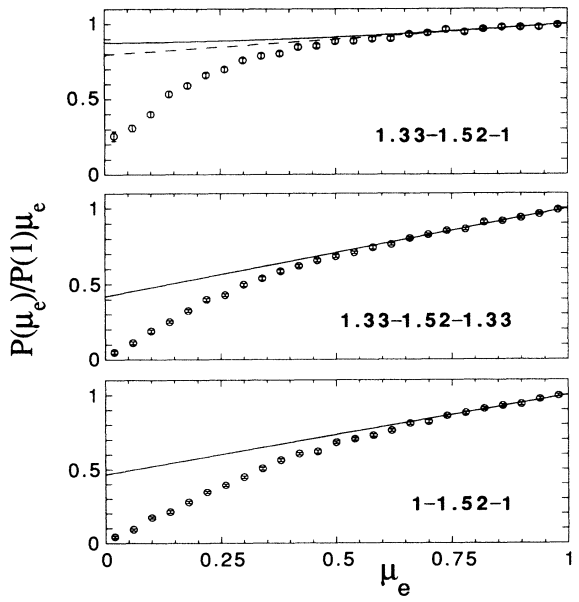

FIG. 6. Angular distribution of photons transmitted through slabs of thickness $L/l^* = 15$ and different interior, wall, and exterior refractive indices as labeled; circles are for simulation results with isotropic scattering. The solid curves represent the diffusion theory prediction, Eq. (4.6) with extrapolation length ratios given in Table I; the dashed line in the top plot shows the leading behavior.

V. CONCLUSIONS

The diffusion theory prediction of Eqs. (1.1) and (2.2) for the probability that a photon which enters a multiple scattering medium will be transmitted rather than backscattered is accurate to approximately 1% for slabs which are sufficiently thick as to be opaque; only for thinner slabs or higher accuracies must radiative transfer theory be invoked in favor of diffusion theory. For opaque samples and accuracies at the 1% level, anisotropy in the scattering events is irrelevant and the only two important physical parameters are the ratio of sample thickness to photon transport mean free path and an average diffuse boundary reflectivity. For a well controlled sample, the latter is accurately given by diffusion theory; for unknown samples, it can be accurately estimated from the leading behavior of the angular distribution of the transmitted light. Thus the systematic error introduced by properly using diffusion theory to analyze transmission experiments in terms of the photon transport mean free path is at the 1% level. By contrast, the procedure outlined in the Introduction can give errors on the order of 10%. The means of achieving the ultimate accuracy of diffusion theory suggested here should be useful for more precise characterization of the structure and dynamics of highly scattering materials using diffuse transmission as well as diffusing-wave spectroscopy.

ACKNOWLEDGMENTS

Thanks are due to J. Rudnick for helpful conversations and D. Weaire for pointing out the cosine dependence in the angular distribution of diffusely transmitted light. We are grateful to both NASA and the Donors of the Petroleum Research Fund, administered by the American Chemical Society, for partial support of this research through Grants Nos. 26967-G9 and NAG3-1419, respectively.

APPENDIX A

The diffusion equation for the density of photons in a slab geometry depends only on the transverse distance z across the sample, and consequently the form of Eq. (1.1)

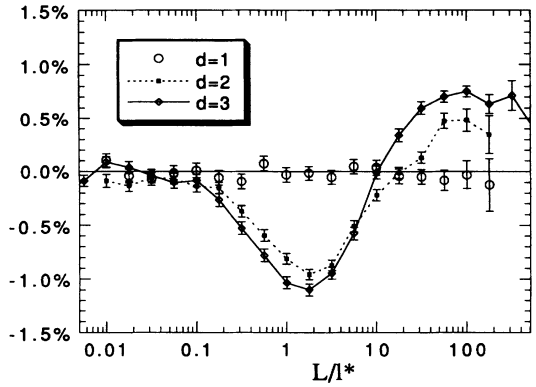

FIG. 7. Percent deviation of simulation results for the diffuse transmission from Eq. (2.4) vs slab thickness in one, two, and three dimensions; extrapolation length ratios are taken from Eq. (A2) as 1, $\pi/4$, and $\frac{2}{3}$, respectively. Note that the deviation increases with dimensionality.

for the transmission probability does not depend on the number, d, of spatial dimensions. The diffuse transmission probability is, nevertheless, affected by dimensionality, but only through the value of the extrapolation length ratio. Consider the flux through an area element at the $z=0$ boundary from photons in a unit volume located a distance r away, and assume that the photon density has an extrapolation length h. Then the diffuse flux through the area element is

$$J_{\text{in,out}} \propto \int_{z<0,z>0} [(h+r\cos\theta)dV]\frac{\cos\theta}{r^{d-1}}\exp(-r/l^*) . \tag{A1}$$

The term in square brackets is proportional to the number of photons in the volume element dV. The next term is proportional to the fraction of photons in that element which are headed toward the area element of interest and the exponential term is the fraction of those which are not scattered before reaching the surface. The integrand has no dependence on the azimuthal coordinates and the relevant part of the volume element is $dV \propto (\sin^{d-2}\theta d\theta)(r^{d-1}dr)$. Integrating separately over each half space and requiring $J_{\text{in}}=RJ_{\text{out}}$ gives

$$z_e(d)=\frac{\sqrt{\pi}\Gamma\left[\frac{d}{2}+\frac{1}{2}\right]}{d\Gamma\left[\frac{d}{2}\right]}\frac{1+R}{1-R} . \tag{A2}$$

For one, two, and three dimensions and $R=0$, the extrapolation length ratios are 1, $\pi/4$, and $\frac{2}{3}$, receptively; for much higher dimensions, $z_e(d)$ vanishes as $\sqrt{\pi/2d}$. According to Eq. (1.1) for the diffuse transmission, then, finite thickness corrections and boundary reflections are more important in lower dimensions.

The accuracy of diffusion theory as a function of dimensionality can be tested by comparison with random walk computer simulations for the case of isotropic scattering and $R=0$. For $d=3$, we average the diffuse transmission results shown in Fig. 2; for $d=1$ and 2, we perform new simulations where steps are taken of length $\Delta s=-l^*\ln\mathcal{N}_{\text{rand}}$ and of direction $\mu=\pm 1$ and $\mu=\cos(2\pi\mathcal{N}_{\text{rand}})$, respectively, where $\mathcal{N}_{\text{rand}}$ is a random number between zero and one and the change in transverse position is $\Delta z=\mu\Delta s$. The percent deviation of simulation results for the diffuse transmission from the diffusion theory prediction of Eq. (2.4) and (A2) is shown in Fig. 7 for a wide range of slab thicknesses. For $d=1$, no deviation is found at the level of about 0.1%; for $d=2$, however, there is deviation outside the single scattering regime which lies between the $d=1$ and the $d=3$ results. We therefore find that the accuracy of diffusion theory decreases with increasing dimensionality.

TABLE II. Diffusion theory predictions and simulation results for the bare extrapolation length ratio when scattering sites are confined to a lattice.

Lattice	z_e prediction	z_e simulation
sc (all d)	1	1.0020±0.0011
Triangular ($d=2$)	$(1+\sqrt{2})/4\cong 0.6036$	0.6059±0.0011
fcc ($d=3$)	$(1+\sqrt{5/3})/4\cong 0.5727$	0.5743±0.0013
bcc ($d=3$)	$(1+\sqrt{11/3})/6\cong 0.4858$	0.4917±0.0012

APPENDIX B

In order to examine the universality of Eqs. (1.1) and (2.2) for the diffuse transmission through a slab geometry, we perform random walk simulations for transport through four different Bravais lattices. In all cases, the lattices are oriented so that the walk starts at one nearest neighbor distance from the edge at $z=0$ and steps are taken to a randomly selected nearest neighbor until the photon lands at a site $z<0$ or $z>L$. Based on the recursion argument presented in Sec. II for the form of Eq. (1.1), we conjecture without further justification that the appropriate extrapolation length equals the average distance outside the sample at which an exiting walker lands. Simulation results for the bare extrapolation length based on the 28 different combinations of seven slab thicknesses $L/l^*=3$, 5, 7, 10, 20, 50, and 100 and four wall reflectivities $R=0$, 0.25, 0.50, and 0.75 are compared with our conjecture in Table II. Agreement is found nearly to within statistical uncertainty for all cases except for the bcc lattice; it is conceivable that Eqs. (1.1) and (2.2) with the conjectured bare extrapolation lengths represent an exact solution. While this may or may not be of mathematical interest if true, the close agreement certainly further demonstrates how robust is the form of Eq. (1.1) for the diffuse transmission through a slab.

[1] A. Ishimaru, *Wave Propagation and Scattering in Random Media* (Academic, New York, 1978). Vol. 1.
[2] S. Fraden and G. Maret, Phys. Rev. Lett. **65**, 512 (1990).
[3] X. Qiu, X.-L. Wu, J. Z. Zhu, D. J. Pine, D. A. Weitz, and P. M. Chaikin, Phys. Rev. Lett. **65**, 516 (1990).
[4] D. J. Durian, D. A. Weitz, and D. J. Pine, Science **252**, 686 (1991).
[5] D. J. Durian, D. A. Weitz, and D. J. Pine, Phys. Rev. A **44**, R7902 (1991).
[6] P. D. Kaplan, A. G. Yodh, and D. J. Pine, Phys. Rev. Lett. **68**, 393 (1992).
[7] J. X. Zhu, D. J. Durian, J. Muller, D. A. Weitz, and D. J. Pine, Phys. Rev. Lett. **68**, 2559 (1992).
[8] A. Meller and J. Stavans, Phys. Rev. Lett. **68**, 3646 (1992).
[9] M. H. Kao, A. G. Yodh, and D. J. Pine, Phys. Rev. Lett. **70**, 242 (1993).
[10] G. Maret and P. E. Wolf, Z. Phys. B **65**, 409 (1987).
[11] D. J. Pine, D. A. Weitz, J. X. Zhu, and E. Herbolzheimer, J. Phys. (Paris) **51**, 2101 (1990).
[12] A. G. Yodh, N. Georgiades, and D. J. Pine, Opt. Commun. **83**, 56 (1991).
[13] F. Liu, K. M. Yoo, and R. R. Alfano, Appl. Opt. **32**, 554 (1993).
[14] D. A. Benaron and D. K. Stevenson, Science **259**, 1463 (1993).
[15] *Scattering and Localization of Classical Waves in Random Media,* edited by P. Sheng (World Scientific, Singapore, 1990).
[16] J. X. Zhu, D. J. Pine, and D. A. Weitz, Phys. Rev. A **44**, 3948 (1991).
[17] J. H. Li, A. A. Lisyansky, T. D. Cheung, D. Livdan, and A. Z. Genack, Europhys. Lett. **22**, 675 (1993).
[18] S. Chandrasekhar, *Radiative Transfer* (Dover, New York, 1960).
[19] T. Klitsner, J. E. Van Cleve, H. E. Fischer, and R. O. Pohl, Phys. Rev. B **38**, 7576 (1988).
[20] E. T. Swartz and R. O. Pohl, Rev. Mod. Phys. **61**, 605 (1989).
[21] R. G. Cole, T. Keyes, and V. Protopopescu, J. Chem. Phys. **81**, 2771 (1984).
[22] K. R. Naqvi, A. El-Shahat, and K. J. Mork, Phys. Rev. A **44**, 994 (1991).
[23] T. M. Nieuwenhuizen and J. M. Luck, Phys. Rev. E **48**, 569 (1993).
[24] G. Placzek and W. Seidel, Phys. Rev. **72**, 550 (1947).
[25] M. Lax, V. Narayanamurti and R. C. Fulton, in *Proceedings of the Symposium on Laser Optics of Condensed Matter,* edited by J. L. Birman, H. Z. Cummins, and A. A. Kaplyanskii (Plenum, New York, 1987), p. 229.
[26] K. M. Yoo, F. Liu, and R. R. Alfano, Phys. Rev. Lett. **64**, 2647 (1990).
[27] W. H. Press, B. P. Flannery, S. A. Teukolsky, and W. T. Vetterling, *Numerical Recipes in C* (Cambridge University Press, New York, 1991), p. 212.
[28] A. Lagendijk, R. Vreeker, and P. De Vries, Phys. Lett. A **136**, 81 (1989).
[29] I. Freund, M. Rosenbluh, and R. Berkovits, Phys. Rev. B **41**, 496 (1990).
[30] M. Born and E. Wolf, *Principles of Optics* (Pergamon, New York, 1983).
[31] D. J. Durian, Bull. Am. Phys. Soc. **38**, 289 (1993).